Title

A long noncoding RNA acts as a post-transcriptional regulator of heat shock protein 70 kDa synthesis in the cold hardy *Diamesa tonsa* under heat shock

Bernabò P.[1,2], Viero G[2], Lencioni V.[1]*

[1] Department of Invertebrate Zoology and Hydrobiology, MUSE-Museo delle Scienze, Corso del Lavoro e della Scienza 3, 38123 Trento, Italy

[2] Institute of Biophysics-CNR Trento Unit, Via Sommarive 18, 38123, Povo, Trento, Italy

* Corresponding author: E-mail valeria.lencioni@muse.it

Running title

Role of lncRNA in heat shock response of *Diamesa tonsa*

Abstract

Cold stenothermal insects living in glacier-fed streams are stressed by temperature variations resulting from glacial retreat during global warming. The molecular aspects of insect response to environmental stresses remain largely unexplored. The aim of this study was to expand our knowledge of how a cold stenothermal organism controls gene expression at the transcriptional, translational, and protein level under warming conditions. Using the chironomid *Diamesa tonsa* as target species and a combination of RACE, qPCR, polysomal profiling, western blotting, and bioinformatics techniques, we discovered a new molecular pathway leading to previously overlooked adaptive strategies to stress. We obtained and characterized the complete cDNA sequences of three heat shock inducible 70 (*hsp70*) and two members of heat-shock cognate 70 (*hsc70*). Strikingly, we showed that a novel pseudo-hsp70 gene encoding a putative long noncoding RNA (lncRNA) which

is transcribed during thermal stress, acting as a ribosome sponge to provide post-transcriptional control of HSP70 protein levels. The expression of the pseudo-hsp70 gene and its function suggest the existence of a new and unexpected mechanism to cope with thermal stress: lowering the pace of protein production to save energy and optimize resources for recovery.

Keywords: Heat Shock Response, gene expression, polysomal profiling, chironomids, climate change

Introduction

Understanding how freshwater species potentially react and adapt to climate change is a major challenge in predicting future biodiversity trends [1]. This is particularly important in high mountain freshwaters where migration and dispersion to escape stressors are hampered by isolation and habitat fragmentation [2, 3, 4]. Owing to shrinking glaciers, water temperature of glacier-fed streams is increasing while their discharge is decreasing, affecting taxonomical and functional diversity of the animal and vegetal communities [5, 6]. Cold stenothermal species adapted to live at temperatures close to their physiological limits might only survive and reproduce if they can adapt to new environmental conditions or if they are able to avoid the stressor adopting specific behaviours [7]. Barring these abilities, they are expected to disappear [8]. In the mountaintop environment exposure is magnified because the rate of warming is amplified with elevation, with high mountain ecosystems experiencing more rapid rate of temperature increase than those in lowlands [9]. Studying the adaptive potential of these species is indeed essential for prediction of the consequences on biota and habitats of global warming in glacierized regions [10].

To detail the molecular response to increased temperature in cold stenothermal species inhabiting glacier-fed streams, we chose *Diamesa tonsa* (Haliday), belonging to the *cinerella* species group (Diptera: Chironomidae). Six Palaearctic species are ascribed to this group, all inhabiting cold running waters, with *D. tonsa* being one of the most common in the Mediterranean Basin as well as Northern Europe and Russia [11]. Larvae of *D. cinerella* gr. are freeze-tolerant, with a thermal optimum below 6 °C [12], and survive short-term heat shock (HS) by developing a Heat Shock Response (HSR) based on the synthesis of Heat Shock Proteins (HSPs) [13].

HSR based on HSPs has been characterized for a wide range of species and found to exhibit a high degree of conservation of its basic properties across prokaryotes and eukaryotes [14]. Under non-stressful conditions HSPs act as molecular chaperones to stabilize actively denaturing proteins, refold proteins that have already denatured, and direct irreversibly denatured proteins to the proteolytic

58 machinery of the cell [15, 16, 17]. Also, under non-stressful conditions HSPs facilitate the correct
59 folding of proteins during translation and their transport across membranes [18, 19]. Among HSPs
60 the 70 kDa family, consisting of inducible (HSP70) and constitutive (heat shock cognate, HSC70)
61 forms, is the most studied in relation to thermal stress and has been found in all organisms
62 investigated to date [20, 21]. [22] and [13] demonstrated that HSC70 plays a role in cold resistance
63 for *D. cinerella* gr. larvae and that the HSR is comprised of a strong transcriptional boost of the
64 inducible HSP70 gene at a temperature six times higher than that at which they live in nature. The
65 involvement of HSC70 and HSP70 in cold and heat tolerance was observed in other cold adapted
66 chironomids such as adults of *Belgica antarctica* [23] and larvae of *Pseudodiamesa branickii* [24].
67 Knowledge of how these insects control gene expression at the transcriptional, translational and
68 protein level under heating is still under-explored. The present study aims to address this using a
69 multi-level approach to study HSR at the transcriptional, translational and protein level in *D. tonsa*.
70 This is particularly important because studying changes in gene expression only at the transcriptional
71 level may be misleading [25, 26] given the poor average correlation between protein and transcript
72 [27, 28] due to post-transcriptional controls of gene expression. Here we hypothesize that, similar to
73 observations in higher eukaryotes, post- transcriptional control of *hsp70* and *hsc70* gene expression
74 in insects may exist. In line with this hypothesis, we identified a novel bio-molecular process in cold
75 adapted organisms, shedding light into a new adaptation strategy to cope with heat stress involving a
76 long noncoding RNA (lncRNA). Intriguingly, over the last few years, lncRNA with putative
77 regulatory function relating to HSR has begun to attract attention, and several of lncRNAs are
78 implicated in mammalian HSR [29]. At present, there are no reports about the involvement of
79 lncRNAs in organisms that, like *D. tonsa,* are actually facing global warming challenges in the wild.
80

81 **Material and Methods**

82 *Animal model and collection*

Fourth-instar larvae of *D. tonsa* were used as an animal model. *D. tonsa* is a Palaearctic species well distributed in the European mountain regions, particularly frequent in the Alps and the Apennines (Fauna Europaea: https://fauna-eu.org/). Larvae were collected with a 30 × 30 cm pond net (100 µm mesh size) in mats of the chrysophyte *Hydrurus foetidus*, in winter 2016, in the glacier-fed stream Frigidolfo (Lombardy Province, NE Italy, 1584 m a.s.l., 10°30′19.32″ N; 46°17′ 51.07″ E). The Frigidolfo stream was characterized by clear (3.8±1.4 Nephelometric Turbidity Unit) and well oxygenated (per cent oxygen saturation= 80% - 90%) waters, with a mean temperature of 4 °C during the sampling period, recorded using a field multiprobe (Hydrolab Quanta, Hydrolab Corporation®, Texas, USA). Larvae were sorted in the field with tweezers, transferred to plastic bottles filled with stream water and transported to the laboratory via cooling bag within 2 hours of collection. Animals were reared in 500-mL glass beaker (max 50 specimens/beaker) with filtered stream water (on Whatman GF/C, particle retention 1.2 µm) in a thermostatic chamber (ISCO, mod. FTD250-plus) at 4 °C with an aerator to maintain oxygen saturation above 80%. The rearing temperature (4 °C) corresponded to the mean environmental temperature during sampling period [24].

Species identification was confirmed by head capsule morphology observed under the stereomicroscope (50 X) according to [30] within 24 h of sampling and by DNA Barcoding analysis of a sub-sample of the collected larvae based on mitochondrial cox1 gene sequence [11].

Heat Shock Exposure

Larvae of *D. tonsa* were exposed for 1 h to three different stress temperatures (15 °C, 26 °C and 32 °C), chosen according to [13]: 26 °C is the highest temperature at which all the tested larvae were found alive after 1 h of stress; 32 °C is the LT_{50} of the larvae in winter season; 15 °C selected as an intermediate temperature between the natural-ideal and sub-lethal temperatures.

3-5 groups of 5 larvae each were transferred to 25-mL plastic bottles (Kartell, Italy) filled with 10 mL of preheated filtered stream water, under aeration to avoid mortality due to oxygen depletion. Larvae were then maintained at the stress temperature for 1 h. In all, 3-5 replicates of 5 specimens each were maintained at 4 °C for the entire period of each treatment and used as control (Ctrl). After treatments, the larvae were returned to 4°C (= rearing temperature) for 1 h and then only living (moving spontaneously) larvae were immediately flash frozen in liquid nitrogen. The larvae were stored at -80 °C until further analyses.

Isolation of total mRNA and reverse transcription

Total RNA was extracted from 2-5 larvae using a commercial kit (TRIZOL, Life Technologies, Carlsbad, CA, USA), according to the manufacturer's protocol. RNA concentration was determined by UV absorption using a NanoDrop ND-1000 spectrophotometer (Thermo Fisher Scientific, Waltham, MA, USA) and quality checked by agarose gel electrophoresis. Total RNA (1 µg) was then reverse transcribed using the First Strand cDNA Synthesis Kit (Thermo Fisher Scientific) and oligo(dT) as primers.

hsp70 amplification

cDNA (1 µL) from control larvae was amplified using the KAPA HiFi HotStart DNA Polymerase Taq (Kapa Biosystems, Wilmington, MA, USA), insect-HSP70 degenerate primers (from Bernabò *et al.*, 2011; Table 1) with a touchdown PCR protocol(annealing from 61 to 50 °C, - 1 °C/cycle + 30 cycles at 50 °C).

PCR product was observed using agarose gel electrophoresis, cloned using the CloneJet PCR Cloning kit (Thermo Fisher Scientific), and transformed into DH5α competent cells. A minimum of 40 colonies were analysed for the presence, size, and sequence of the PCR insert using colony PCR-RFLP analysis (TRu1 l restriction enzyme). Three different electrophoresis restriction patterns were

132 observed, and the corresponding inserts were sequenced.

133

134 *5′ and 3′ RACE PCR*

135 Amplification of 5′ and 3′ ends of cDNA was performed according to the protocol described in the
136 SMART RACE cDNA Amplification Kit (Takara Bio USA, Inc. Mountain View, CA, USA). Three
137 pairs of gene-specific primers (GSP), one for each hsp70 isoform: *hsp70, hsc70-I* and *hsc70-II*, were
138 designed based on the sequences obtained from amplification with degenerate primers (Table 1).
139 Total RNA of *Diamesa tonsa* larvae was extracted according to the Trizol protocol (Thermo Fisher
140 Scientific) and the quantity and quality assessed as described above. 1 µg of total RNA was first
141 retrotranscribed with primers supplied in the kit and this first-strand cDNA was used directly in PCR
142 amplification reactions that were achieved using a high-fidelity enzyme (KAPA HiFi DNA
143 Polymerase, Kapa Biosystems), the Universal Primer Short (UPS, supplied by the kit), and gene-
144 specific primer (GSP_F for 3′ RACE- cDNA or GSP_R for 5′ RACE- cDNA). The PCR was
145 performed with the following cycler protocol: 95 °C for 3 min, 25 cycles of 98 °C for 30 sec, 68 °C
146 for 15 sec and 72 °C for 90 sec, and a final extension of 5 min at 72 °C.

147

148 *Cloning and sequencing of 5′ and 3′-RACE PCR products*

149 PCR products were run and purified by agarose gel electrophoresis and cloned into the pJET 1.2
150 cloning vector (Thermo Fisher Scientific). The inserts were sequenced.

151

152 *Sequences analysis*

153 Full-length cDNA sequences have been deposited in GenBank under accession numbers KC860254
154 (*Dc-hsp70*), KC860255 (*Dc-hsc70-I*) and KC860256 (*Dc-hsc70-II*). When sequences were deposited,
155 they were ascribed to a *Diamesa cinerella* gr., referred to as *Dc-*, only successively was the species
156 identification confirmed as *D. tonsa*. Throughout the paper we decided to refer the genes to the

157 species "tonsa" as *Dt-*. The sequences were used to search for homology in other organisms by
158 BLAST software on the NCBI website (https://blast.ncbi.nlm.nih.gov/Blast.cgi).
159 Sequence alignments were carried out using the Bioedit software package and ORFs were identified
160 with the aid of the software ORF Finder (http://www.ncbi.nlm.nih.gov/projects/gorf/). Molecular
161 weights of the predicted proteins were calculated by Compute pI/Mw tool (ExPASy)
162 (http://web.expasy.org/compute_pi/). The phylogenetic trees were constructed using the "One Click"
163 mode with default settings in the Phylogeny.fr platform (http://www.phylogeny.fr) [31].
164 The presence of possible splicing sites was predicted using the BDGP: Splice Site Prediction by
165 Neural Network (http://www.fruitfly.org/seq_tools/splice.html).
166 Specific primers for expression analysis were designed from the full-length cDNA sequences of *Dt-*
167 *hsp70*, *Dt-hsc70I* and *Dt-hsc70II* (Table 1) using Primer3Web (http://primer3.ut.ee) and OligoCalc
168 (http://biotools.nubic.northwestern.edu/OligoCalc.html).
169
170 *Polysomal extraction*
171 Polysomes were extracted as reported in [26]. Briefly, 5 frozen larvae were pulverized under liquid
172 nitrogen in a mortar with a pestle and the powder lysed in 0.8 mL of lysis buffer (10 mM Tris-HCl at
173 pH 7.5, 10 mM NaCl, 10 mM $MgCl_2$, 1% Triton-X100, 1% Na- deoxycholate, 0.4 U/µL
174 SUPERase.In RNase Inhibitor (Life Technologies), 1 mM DTT, 0.2 mg/mL cycloheximide, 5 U/mL
175 Dnase I). Following lysis, cellular debris was removed by centrifugation (13.200 rpm, 2 min at 4 °C)
176 and the supernatant was kept ice-cold for 15 minutes. The cleared lysate was then centrifuged at
177 13.200 rpm, 5 min at 4 °C to remove all nuclei and mitochondria. The supernatant obtained was
178 layered onto a 12 mL linear sucrose gradient (15%–50% sucrose [w/v], in 30 mM Tris-HCl at pH
179 7.5, 100 mM NaCl, 10 mM $MgCl_2$) and centrifuged in a SW41Ti rotor (Beckman) at 4 °C and
180 197.000 *g* for 100 min in a Beckman Optima LE-80K Ultracentrifuge. 1 mL fractions were collected
181 with continuous absorbance monitoring at 254 nm using an ISCO UA-6 UV detector.

182

183 *Polysomal RNA extraction*

184 Sucrose fractions from the entire polysomal profile were divided into two groups (subpolysomal and
185 polysomal fractions) and the pooled fractions were treated with 1% SDS and proteinase K (100
186 µg/mL) for 75 minutes at 37 °C before phenol–chloroform RNA extraction. Polysomal RNA pellet
187 was resuspended in 25 µL of Rnase-free water. RNA was quantified by Nanodrop and the quality
188 was assessed by agarose gel electrophoresis.

189

190 *Quantitative real-time RT-PCR (qPCR)*

191 Subpolysomal and polysomal RNA (500 ng) was reverse transcribed using the First Strand cDNA
192 Synthesis Kit (Thermo Fisher Scientific) following the manufacturer's instructions. cDNA was
193 amplified by Real-Time PCR using Kapa Sybr Fast qPCR Mastermix (Kapa Biosystems) and
194 specific primers (Table 1) on a CFX96 Touch™ Real-Time PCR Detection System (Biorad,
195 Hercules, CA, USA). *Actin* was used as housekeeping gene normalization control (Table 1). For each
196 condition, 3 biological replicates were prepared, and for each biological replicate, 3-4 Real-Time
197 PCR amplifications were run. Each primer pair was validated for dimer formation by melting curve
198 analysis. Amplification profiles were analysed using CFX Manager Software (analysis of the melting
199 Curve for the presence of primer dimer) and relative expression levels were calculated using the
200 delta/delta Ct method [32]. The log2 ΔTE (change of Translation Efficiency) was calculated as the
201 ratio between the fold change at the polysomal level and the fold change at the sub-polysomal level
202 of the gene of interest.

203

204 *Protein extraction and Western Blot analysis*

205 Protein was extracted from 5 live larvae using the methanol/chloroform protocol [33] and solubilized
206 in electrophoresis sample buffer (Santa Cruz Biotechnology, Dallas, TX, USA) for SDS-

polyacrylamide gel electrophoresis and Western Blot analysis. Gel electrophoresis was performed using 12% Mini-PROTEAN-TGX Precast Protein Gels (Bio-Rad) and transferred to nitrocellulose membrane. Immunoblotting was performed using GAPDH (1:1,000, Santa Cruz Biotechnology) and HSP70 (1:800, Abcam, Cambridge, UK) primary antibodies and the corresponding HRP-conjugated secondary antibodies (1:2,000, Santa Cruz Biotechnology). The blots were developed with SuperSignal™ West Femto Maximum Sensitivity Substrate (Thermo Fisher Scientific) and acquired on a ChemDoc-It (BioRad Laboratories). The image analysis was performed using the ImageJ (https://imagej.nih.gov/ij/) image processing package.

Genomic DNA extraction and amplification

Genomic DNA was extracted from a single larvae of *D. tonsa* using the DNeasy Blood & Tissue Kit (Qiagen, Hilden, Germany), following the manufacturer's instructions. The gDNA concentration was estimated by Qubit and about 20 ng of gDNA amplified with primers specifically designed to include the intron region (Hsp70 genomic F/R, Table 1) using PuReTaq Ready-To-Go™ PCR Beads (GE Healthcare, Chicago, IL, USA).

Gene copy number analysis

The relative copy number for *hsp70* with and without intron was estimated by Real-Time PCR analysis using SYBR Green dye. Two pairs of primers that specifically recognize *hsp70 with intron* (Intron-F and Intron-R, Table 1) or *hsp70 without intron* (Hsp70 no intron-F and Hsp70 no intron-R, Table 1) were used to amplify gDNA by Real-Time PCR using qPCRBIO SyGreen Mix Separate-ROX (PCR Biosystem, Wayne, PA, USA) with Mic qPCR Cycler (Bio Molecular System, Upper Coomera, Australia). Consistent efficiency of the two primer pairs was analysed by the amplification of a serial dilution of gDNA. Four different larvae gDNAs were amplified and the ΔCt between the

231 *hsp70* and the *hsp70 + intron* signal calculated. The Relative Gene Copy Number was finally
232 calculated using $2^{\Delta Ct}$.
233
234 **Results**
235 *Cloning, sequencing, and characterization of the Dt-hsp70 transcripts*
236 For detailed study of the HSR of *Diamesa tonsa*, we produced the complete sequences of *hsp*
237 transcripts in this organism. We cloned the *hsp* transcripts, using degenerate primers based on a
238 conserved region of insect's *hsp70,* and performed RACE PCR to amplify cDNAs. With this
239 approach we successfully obtained sequences for three unique transcripts (Figure 1A and
240 Supplementary Figures 1, 2). The nucleotide sequence of the first transcript was highly homologous
241 to the well-known *hsp70* inducible isoform (Figure 1A, *Dt-hsp70*). The remaining transcripts were
242 likely the constitutive isoforms *(*Supplementary Figures 1, 2, *Dt-hsc70-I, Dt-hsc70-II)*.
243 Upon performing a cross-species alignment, we found that the cDNA sequence of *Dt-hsp70* shared
244 high homology with other inducible *hsp70s* from other insects: 81% with *Chironomus yoshimatsui*
245 (AB162946.1) and 72% with *Phenacoccus solenopsis* (KM221884.1), strongly suggesting that this
246 transcript indeed belongs to the *hsp70* family. The *Dt-hsc70-I* showed high homology with
247 constitutive form *hsp70* from other Diptera: 82% with both *Sitodiplosis mosellana* (KM014659.1)
248 and *Polypedilum vanderplanki* (HM589530.1). Similarly, we found that *Dt-hsc70-II* shared the
249 highest homology with *P. vanderplanki* (HM589531.1) and *Acyrthosiphon pisum*
250 (NM_001162948.1).
251 The alignment of deduced amino acid protein sequences resulted in characteristic hsp70 family
252 motifs, further supporting our hypothesis that these transcripts are *bona fide* products of the hsp70
253 gene (Figure 1A and Supplementary Figure 1A). In particular, we found the motifs IDLGTTYS,
254 DLGGGTFD, and IVLVGG and the cytoplasmic *hsp70* carboxyl-terminal region (EEVD) in the case
255 of *Dt-hsp70* and *Dt-hsc70-I*. In *Dt-hsc70-II* we also found the characteristic ER localization signal

(KDEL) at the C-terminus (Figure 1A and Supplementary Figure 1A). A summary of the characteristics of all sequences and their deduced proteins is displayed in Table 2.

Next, using both the nucleotide and the amino acid sequence of *Dt-hsp70,* we obtained two phylogenetic trees (Figure 1B and 1C). Interestingly, *Dt-hsp70* clustered with the *hsp70* of the closely related chironomids (*Chironomus* spp). The relationships displayed in the trees were in agreement with established Diptera phylogeny, with chironomids separated from other Nematocera and Brachycera [34, 35]. Similar results were obtained for *Dt-hsc70-I* and *Dt-hsc70-II* using the Phylogeny.fr tool on the ExPASy Proteomics server [31] (Supplementary Figure 2).

Identification of a novel hsp70-pseudogene encoding a putative lncRNA

While analysing the response of the *Dt-hsp70* transcript to heat stress for 1 h and at 15°, 26°, and 32 °C and using primers for *Dt-hsp70*, we serendipitously observed that two amplicons were produced from cDNA amplification (Figure 2A and Table 1). The unexpected second PCR amplicon was about 400 bp longer than the expected one and was observed exclusively in larvae exposed to heat stress. Intrigued by these results, we cloned and sequenced this alternative transcript and compared it to *Dt-hsp70* (Supplementary Figure 3). This alternative transcript has a short intron of 404 bases (from nucleotide 421 to 854, donor site from nucleotide 421 to 435 [*prediction score* = 0.96]; acceptor score from nucleotide 835 to 875 [*prediction score* = 0.98]) and a polyA tail following nucleotide 1239. In human, hsp70 pseudogenes can act as long nc-RNAs. Thus, we suspected this novel transcript to have similar characteristics. To test this hypothesis, we used a computational prediction tool [36] to calculate the probability of our novel transcript being a lncRNA. As control we used the same tool on the *Dt-hsp70* transcript and obtained that *Dt-hsp70* is classified as a coding transcript with coding probability 1, Fickett score 0.41216, complete putative ORF of 635 aa in length, and a pI 5.67, in agreement with data shown in Table 2. Strikingly, the

novel Hsp70 transcript was classified as a noncoding sequence with coding probability 0.300294, Fickett score 0.36989, a complete putative ORF of 110 aa, and a pI 8.70.

Next, we wanted to understand if this transcript represents an additional isoform of the hsp70 gene or an as yet uncharacterized gene. To answer this question we extracted genomic DNA from *D. tonsa* larvae and probed using primers that include the additional sequence, 404 bp long. The amplification clearly showed two bands (Figure 2B). The shorter band was about 300 bp long while the longer band and fainter band was observed at about 700 bp, i.e. the difference in the length is exactly what we would expect in the case of two genes. This result suggests that these two transcripts are associated with two different genes in the *D. tonsa* genome. To further prove that this is the case, we calculated the relative intensity of the two bands, finding the *Dt-hsp70* to be exactly two-fold more intense than the alternative transcript (Figure 2C). This result suggests that two independent genes encode these transcripts. Moreover, these genes are represented at different copy number in the genome as demonstrated by the Gene Copy Number analysis by qPCR (Figure 2C).

Summarizing these results, we found that: i) in addition to the hsp70 gene, *D. tonsa* has a putative *hsp* pseudogene; ii) this gene encodes at least one transcript containing an insertion with respect to the *Dt-hsp70*; iii) the transcript has a partial overlap with the full length *Dt-hsp70*; iv) this transcript is likely a lncRNA. Given these characteristics, we named this gene *Dt-Ps-hsp70*.

Multi-level analysis of changes in gene expression during thermal stress

To address the question of how *D. tonsa* adapts to thermal stress at the molecular level, we studied the gene expression changes in *Dt-hsp70*, *hsc70-I*, and *hsc70-II* induced by high temperature (15, 26, and 32 °C) in mature larvae. We hoped to set up the most complete experimental design to date for this organism and addressed the question by monitoring changes at the transcriptional, translational, and protein levels (Figure 3A). We extracted total RNA, polysome-associated RNA, and proteins from larvae exposed to 15, 26, and 32 °C. We studied all three levels of gene expression in the case

of *Dt-hsp70* and the transcriptional and translational level for *Dt-hsp70-I* and *II*.

We found that *Dt-hsp70* and *Dt-hsc70-I* were significantly up regulated at 26 and 32 °C ($p < 0.001$), while a slight, but still statistically significant, decrease was observed for *Dt- hsc70-II* at 26 °C (Figure 3B). The most dramatic transcriptional changes were observed for *Dt-hsp70*. A slight but significant positive change was observed in *Dt- hsc70-I* at 26 and 32 °C. *Dt- hsc70-II* did not change its recruitment on polysomes (Figure 3C). Interestingly *Dt-hsp70* showed strong variability among the four thermal stresses, with a decrease in mRNA recruitment at 15 °C ($p < 0.001$) and an increase at 32 °C ($p < 0.001$) (Figure 3C). Interestingly, at 26 °C, when the transcriptional up-regulation is at its maximal level (Figure 3B), no changes were observed at the polysomal (i.e. translational) level. This result suggests that, despite robust transcriptional activation, the protein is likely not produced. To test this hypothesis, we focused our attention on this transcript and studied the protein level by Western Blotting from total protein extracts (Figure 3D). GAPDH was used as protein loading control. HSP70 protein densitometry analysis clearly shows a trend which resembles the observed translational changes. Next, we compared the changes at all three levels (Figure 3E) and found that the fold-change profiles of protein and translational level were similar showing very high correlation ($R^2 = 0.922$, Figure 3E, inset). Conversely, the profile of the transcriptional fold-change clearly differs, with no change at 15 °C and remarkable increase at 26 and 32 °C, and very low correlation with the translational level ($R^2 = 0.389$; Supplementary Figure 4A).

Role of Dt-Ps-hsp70 in translational control of HSP70 protein expression

Having shown that at 26 °C of thermal stress there is a strong uncoupling of transcription and translation/protein level, we wondered whether, similar to observations in mammals during heat stress [29], the putative lncRNA *Dt-Ps-hsp70* transcript plays a role in attenuating the transcriptional boost.

329 To test this hypothesis, we studied the changes of *Dt-Ps-hsp70* at both the transcriptional and
330 translational level by qPCR (Figure 4A and B), using conveniently designed primers (Supplementary
331 Figure 4B and Table 1). An increase in the expression of *Dt-Ps-hsp70* at transcriptional level was
332 detected at 26 °C and 32 °C ($p < 0.001$) (Figure 4A), similar to observations of *Dt-hsp70* (Figure
333 3B).
334 This transcript was uploaded on polysomes, with a positive fold-change with respect to the control,
335 exclusively at 26 °C (Figure 4B). Next, we calculated the relative variations of translational and
336 transcriptional changes (Translation Efficiency (ΔTE) in Figure 4C). A statistically significant
337 increase in the ΔTE was observed in larvae stressed at 26 °C ($p < 0.001$) and 32 °C ($p < 0.05$).
338 Strikingly, the most robust up-regulation was at 26 °C, precisely when we observed the strongest
339 uncoupling of transcription and translation in *Dt-Ps-hsp70* (Figure 4D).
340 Taken together these results suggest that the *Dt-Ps-hsp70* transcript likely competes with the *Dt-*
341 *hsp70* transcript for ribosome recruitment, leading to attenuation of the global efficiency of HSP70
342 production at 26 °C and suggesting that *Dt-Ps-hsp70* acts as a ribosome sponge to modulate the
343 protein synthesis of HSP70.
344

345 **Discussion**

346 The HSR is an important biochemical indicator for assessing levels of thermal stress and thermal
347 tolerance limits stemming from the fact that protein conformation is a thermally sensitive weak-link
348 [17]. Thus, species sensitivity inferred from HSR activation might be used as a proxy of their
349 ecological valency [e.g., 23, 37, 38, 39] and their vulnerability to climate change.
350 Under HS, the cold adapted *D. tonsa* deploys a molecular strategy involving HSR (Figure 5). This
351 strategy appears more complex than previously considered for larvae of *Diamesa* [13, 22] and other
352 Diamesinae [22]. One *hsp70* gene (*Dt-hsp70*), one pseudogene *hsp70* (*Dt-Ps-hsp70*) and two
353 isoforms of *hsc70* (*Dt-hsc70-I* and *Dt-hsc70-II*) have been sequenced in *D. tonsa*, experimentally

354 showing differential expression under increased temperature (15, 26 and 32 °C). This response was
355 studied here at the transcriptional, translational, and protein level. As expected [22], *D. tonsa* showed
356 strong activation of transcription of *hsp70* inducible forms (*Dt-hsp70*) at temperatures ≥ 26 °C, and,
357 to a minor extent, also of the cytoplasmic constitutive form (*Dt-hsc70-I*) at both 26 and 32 °C. We
358 found that *Dt-hsp70* and *Dt-hsc70-I* were significantly up-regulated at 26 and 32 °C, whilst a slight,
359 still statistically significant decrease was observed for *Dt- hsc70-II* at 26 °C. In accordance with
360 previous findings by other co-authors [40], the strongest transcriptional changes were observed for
361 *Dt-hsp70*. Overall, *Dt-hsc70-I* cooperates with *Dt-hsp70* to help *D. tonsa* larvae survive stress.
362 The presence of more than one member of the *hsc70* family has been previously observed in other
363 insects. For example, in the mosquito *Culex quinquefasciatus* [41] and the fruit fly *Drosophila*
364 *melanogaster* [42] the hsp70 family includes seven heat shock cognate genes (*hsc70-1-7*). These
365 genes are all expressed during normal growth, but the proteins show different subcellular
366 localization: *hsc70-x* localizes to mitochondria, *hsc70-3* to the endoplasmic reticulum (ER) and the
367 others either to the cytoplasm or the nucleus [43]. Phylogenetic analysis suggests that the cDNA
368 sequences of *Dt-hsp70* and *Dt-hsc70-I* are more similar to those obtained from other Chironomidae
369 than to other Diptera families. Conversely *Dt-hsc70-II* clusters with the *hsc70* of *Aedes aegypti*
370 (Culicidae) and *hsc70-3* of *D. melanogaster* (Drosophilidae). This is probably due to the different
371 subcellular localization of this *hsc70* member: *hsc70* of *Aedes aegypti* and *hsc70-3* of *D.*
372 *melanogaster* correspond to proteins localized in the ER and both presented the Hsp70 C-terminal
373 ER localization signal (KDEL) [43, 44] as does *Dt-hsc70-II*.
374 The discovery of a putative *hsp* pseudogene that encodes for at least one transcript containing an
375 intron with respect to the *Dt-hsp70*, and its prediction as a lncRNA, is a very intriguing finding. *Dt-*
376 *hsp70,* which is an inducible *Hsp70* gene, is intron-less as is typical in most organisms. As such, it
377 does not require splicing for normal function [40, 45]. The lack of introns enables the transcribed
378 mRNAs to move rapidly from the nucleus to the cytoplasm without splicing, significantly

accelerating the HSR. Notably, splicing machinery is usually strongly inhibited by HS and other stressors. This fact may favour the selection of intron-less copies of *hsp* genes in the course of evolution [46, 47]. Introns have been considered to appear more frequently in cognate isoforms expressed at normal temperatures [48]. There are, however, several exceptions to this rule, such as in several species of fungi [49, 50], plants [51, 52], the nematode *Caenorhabditis elegans* [53], and in the grasshopper *Locusta migratoria* [54]. Interestingly, in these organisms, *hsp70* genes with introns were constitutively expressed [54]. Specifically, in *C. elegans*, with intron-exon arrangement of *hsp* genes, the splicing of *Hsp70* mRNA occurs with maximal efficiency after moderate HS while splicing of "normal" cellular genes, such as tubulin, is concomitantly blocked by a still unknown mechanism [55].

As has been reported for long noncoding RNAs of mammals [56], the *Dt-Ps-hsp70* transcript was uploaded on polysomes with a positive fold-change exclusively at 26 °C. Strikingly, the most robust up-regulation was at 26 °C, precisely when we observed the strong uncoupling of transcription and translation for the pseudogene. The fact that *Dt-Ps-hsp70* shares with *Dt-hsp70* the first half of the sequence leads us to propose a possible mechanism to explain the transcriptional/translational uncoupling and low protein production of HSP70 at 26 °C. Having the same 5′ sequence, it is reasonable that both transcripts have very similar probability of translation initiation events. This means that *Dt-Ps-hsp70* transcript can compete with the *Dt-hsp70* transcript for ribosome engagement. This condition can control the global efficiency of HSP70 production at 26 °C, suggesting that *Dt-Ps-hsp70* acts as a ribosome sponge and translational modulator of HSP70 protein levels. The uncoupling of transcription and translation can be explained by the consideration that, while important in facilitating tolerance of heat stress, the synthesis of HSPs has considerable metabolic costs, and it is activated only when essential for survival, otherwise it might be maladaptive [17]. Translation is known to drain more cellular energy than transcription [57]. The synthesis of HSPs, and their function as ATP-consuming chaperones in protein folding reactions, can

404 add considerably to the ATP demands of the cell, explaining the repression of basal transcription and
405 translation [21]. Furthermore, our findings emphasize that transcription alone is not necessarily a
406 reliable final readout of HSR in *D. tonsa*.
407 Consistent with our results, unspliced mRNAs are uploaded on polysomes for translation, resulting in
408 the production of a pool of abnormal (truncated) Hsp70 proteins [58]. This finding emphasized that
409 in this chironomid, as in many organisms from yeast [46, 49] and plants [52] to humans [59],
410 exposure to heat does affect the spliceosome and hinders intron splicing .
411 The lncRNA discovered in *D. tonsa* is employed as a means of gene regulation and control of HSP70
412 synthesis under warming stress, as typically observed in higher eukaryotes, predicted by Jacob and
413 Monod 58 years ago [60] and demonstrated in mammals [29].
414 Recently, great attention has been paid to lncRNAs that should not act as protein-coding transcripts
415 but are still found associated with polysomes for largely unknown function [61]. The literature
416 suggests that the majority of the genomes of mammals and other complex organisms is in fact
417 transcribed into lncRNAs (including those derived from introns), many of which are alternatively
418 spliced and/or processed into smaller products [61]. At present, there are no clues about the
419 involvement of lncRNAs in cold stenothermal organisms that are facing global warming challenges
420 in the wild, such as *D. tonsa*. In this species, the gene encoding the lncRNA was preserved in the
421 genome but is never expressed under natural conditions.
422 Our findings highlight for the first time the existence and the putative function of a lncRNA in HSR
423 in a cold stenothermal insect. Why was an *hsp70* pseudogene positively selected by evolutionary
424 driving forces? An attractive hypothesis is that the presence of inducible intron-isoforms could
425 reflect an evolutionary strategy and adaptation to survive heat shock in cold adapted organisms,
426 living constantly in cold waters [62]. Future experiments will be necessary to test this.
427

428 **Acknowledgements**

We thank Alessandra Franceschini and Francesca Paoli (MUSE-Museo delle Scienze of Trento) for animal collection.

Competing interests

The authors declare no competing or financial interests.

Author contributions

Conceptualization: V.L.; Formal analysis: P.B.; Investigation: P.B. and V.L.; Supervision V.L. and G.V.; Writing—Original Draft Preparation: P.B.; Writing—Review and Editing: V.L. and G.V.

References

1. Jeremias G, Barbosa J, Marques SM, Asselman J, Gonçalves FJM, Pereira JL. Synthesizing the role of epigenetics in the response and adaptation of species to climate change in freshwater ecosystems. Mol Ecol. 2018;27(13):2790-2806. https://doi.org/10.1111/mec.14727

2. Woodward G, Perkins DM, Brown LE. Climate change and freshwater ecosystems: Impacts across multiple levels of organization. Philos Trans R Soc Lond B Biol Sci. 2010;365(1549):2093-2106. https://doi.org/10.1098/rstb.2010.0055

3. Lencioni V, Spitale D. Diversity and distribution of benthic and hyporheic fauna in different stream types on an alpine glacial floodplain. Hydrobiologia. 2015;751:73-87. https://doi.org/10.1007/s10750-014-2172-2

4. Hotaling S, Finn DS, Joseph Giersch J, Weisrock DW, Jacobsen D. Climate change and alpine stream biology: progress, challenges, and opportunities for the future. Biol Rev Camb Philos Soc. 2017;92:2024-2045. https://doi.org/10.1111/brv.12319

5. Milner AM, Khamis K, Battin TJ, Brittain JE, Barrand NE, Fuereder L et al. Glacier shrinkage driving global changes in downstream systems. Proc Natl Acad Sci U S A. 2017;114(37):9770-9778. https://doi.org/10.1073/pnas.1619807114

6. Brown L, Khamis K, Wilkes M, Blaen P, Brittain J, Carrivick J, et al. Globally consistent responses of invertebrates to environmental change. Nat Ecol Evol 2018;2(2):325-333. https://doi.org/10.1038/s41559-017-0426-x

7. Pallarés S, Millán A, Mirón JM, Velasco J, Sánchez-Fernández D, Botella-Cruz M et al. Assessing the capacity of endemic alpine water beetles to face climate change. Insect Conserv Divers. 2019. https://doi.org/10.1111/icad.12394

8. Lencioni V. Glacial influence and macroinvertebrate biodiversity under climate change: lessons from the Southern Alps. Sci Total Environ. 2018;622-623:563-575. https://doi.org/10.1016/j.scitotenv.2017.11.266

9. Wang Q, Fan X, Wang M. Recent warming amplification over high elevation regions across the

465 globe. Clim Dyn. 2014;43:87-101. https://doi.org/10.1007/s00382-013-1889-3

466 10. Lencioni V, Bernabò P. Thermal survival limits of young and mature larvae of a cold
467 stenothermal chironomid from the Alps (Diamesinae: *Pseudodiamesa branickii* [Nowicki, 1873]).
468 Insect Sci. 2017;24(2):314-324. https://doi.org/10.1111/1744-7917.12278

469 11. Montagna M, Mereghetti V, Lencioni V, Rossaro B. Integrated Taxonomy and DNA Barcoding
470 of Alpine Midges (Diptera: Chironomidae). PLoS One. 2016;11(7):e0159124. https://doi.org/
471 10.1371/journal.pone.0149673

472 12. Lencioni V, Bernabò P, Jousson O, Guella G. Cold adaptive potential of chironomids
473 overwintering in a glacial stream. Physiol Entomol. 2015;40:43-53.
474 https://doi.org/10.1111/phen.12084

475 13. Lencioni V, Bernabò P, Cesari M, Rebecchi L. Thermal stress induces hsp70 proteins synthesis
476 in larvae of the cold stream non-biting midge *Diamesa cinerella* Meigen. Arch Insect Biochem
477 Physiol. 2013;83:1-14. https://doi.org/10.1002/arch.21088

478 14. Feder ME, Hofmann GE. Heat-shock proteins, molecular chaperones, and the stress response:
479 evolutionary and ecological physiology. Annu Rev Physiol. 1999;61:243-82.
480 https://doi.org/10.1146/annurev.physiol.61.1.243

481 15. Morimoto RI, Kline MP, Bimston DN, Cotto JJ. The heat-shock response: regulation and
482 function of heat-shock proteins and molecular chaperones. Essays Biochem. 1997;32:17-29.

483 16. Glickman MH, Ciechanover A. The ubiquitin-proteasome proteolytic pathway: destruction for
484 the sake of construction. Physiol Rev. 2002;82:373-428.
485 https://doi.org/10.1152/physrev.00027.2001

486 17. Tomanek L. Variation in the heat shock response and its implication for predicting the effect of
487 global climate change on species' biogeographical distribution ranges and metabolic costs. J Exp
488 Biol. 2010;213:971-979. https://doi.org/10.1242/jeb.038034.

489 18. Lindquist S, Craig E. The Heat-Shock Proteins. Annu Rev Genet. 1988;22:631-677.

https://doi.org/10.1146/annurev.ge.22.120188.003215

19. Hartl FU, Hayer-Hartl M. Molecular chaperones in the cytosol: from nascent chain to folded protein. Science. 2002;295:1852-1858. https://doi.org/10.1126/science.1068408

20. Gupta RS, Golding GB. Evolution of HSP70 gene and its implications regarding relationships between archaebacteria, eubacteria, and eukaryotes. J Mol Evol. 1993;37(6):573-82. https://doi.org/10.1007/bf00182743

21. Chen B, Feder M E, Kang L. Evolution of heat-shock protein expression underlying adaptive responses to environmental stress. Mol Ecol. 2018;27:3040-3054. https://doi.org/10.1111/mec.14769

22. Bernabò P, Jousson O, Latella L, Martinez-Guitarte JL, Rebecchi L, Lencioni V. Comparative analysis of Heat shock proteins and thermoresistance in stenothermal insects from caves and cold streams (NE, Italy). Comp Biochem Physiol A Mol Integr Physiol. 2009;154:S4. https://doi.org/10.1016/j.cbpa.2009.05.023.

23. Rinehart JP, Hayward SAL, Elnitsky MA, Sandro LH, Lee RE, Denlinger DL. Continuous up-regulation of heat shock proteins in larvae, but not adults, of a polar insect. Proc Natl Acad Sci U S A. 2006;103:14223-14227. https://doi.org/10.1073/pnas.0606840103

24. Bernabò P, Rebecchi L, Jousson O, Martínez-Guitarte JL, Lencioni V. Thermotolerance and hsp70 HSR in the cold-stenothermal chironomid *Pseudodiamesa branickii* (NE Italy). Cell Stress Chaperones. 2011;16:403-410. https://doi.org/10.1007/s12192-010-0251-5

25. Tebaldi T, Re A, Viero G, Pegoretti I, Passerini A, Blanzieri E, Quattrone A. Widespread uncoupling between transcriptome and translatome variations after a stimulus in mammalian cells. BMC Genomics. 2012;13:220. https://doi.org/10.1186/1471-2164-13-220

26. Bernabò P, Lunelli L, Quattrone A, Jousson O, Lencioni V. Viero G. Studying translational control in non-model stressed organisms by polysomal profiling. J Insect Physiol. 2015;76:30–35. https://doi.org/10.1016/j.jinsphys.2015.03.011

515 27. Schwanhausser B, Busse D, Li N, Dittmar G, Schuchhardt J, Wolf J et al. Global quantification
516 of mammalian gene expression control. Nature. 2011;473:337-342.
517 https://doi.org/10.1038/nature10098
518 28. Vogel C, De Sousa Abreu R, Ko D, Le SY, Shapiro BA, Burns SC et al. Sequence signatures and
519 mRNA concentration can explain two-thirds of protein abundance variation in a human cell line.
520 Mol Syst Biol. 2010;6:400. https://doi.org/10.1038/msb.2010.59
521 29. Place RF, Noonan EJ. Non-coding RNAs turn up the heat: An emerging layer of novel regulators
522 in the mammalian heat shock response. Cell Stress Chaperones. 2014;19(2):159–172.
523 https://doi.org/10.1007/s12192-013-0456-5
524 30. Rossaro B, Lencioni V. A key to larvae of species belonging to the genus *Diamesa* from Alps
525 and Apennines (Italy). Eur J Environ Sci. 2015;5(1):62-79.
526 https://doi.org/10.14712/23361964.2015.79
527 31. Dereeper A, Guignon V, Blanc G. Phylogeny.fr: robust phylogenetic analysis for the non-
528 specialist. Nucleic acids Res 2008;36:W465-W469. https://doi.org/10.1093/nar/gkn180
529 32. Schmittgen TD, Livak KJ. Analyzing real-time PCR data by the comparative CT method. Nat
530 Protoc. 2008;3:1101-1108. https://doi.org/10.1038/nprot.2008.73
531 33. Wessel D, Flügge UI. A method for the quantitative recovery of protein in dilute solution in the
532 presence of detergents and lipids. Anal Biochem. 1984;138:141-143.
533 https://doi.org/10.1016/0003-2697(84)90782-6
534 34. Friederich M, Tautz D. Evolution and phylogeny of the Diptera: a molecular phylogenetic
535 analysis using 28S rDNA sequences. Syst Biol. 1997;46(4):674-698.
536 https://10.1093/sysbio/46.4.674
537 35. Oesterbroek FLS, Courtney G. Phylogeny of the nematocerous families of Diptera (Insecta). Zool
538 J Linn Soc. 1995;115:267-311. https://10.1111/j.1096-3642.1995.tb02462.x
539 36. Kang Y-J, Yang D-C, Kong L, Hou M, Meng Y-Q, Wei Let al. CPC2: a fast and accurate coding

potential calculator based on sequence intrinsic features. Nucleic Acids Res. 2017;45(W1):W12-W16. https://doi.org/10.1093/nar/gkx428

37. Bosch, TC, Krylow, SM, Bode, HR, Steele, RE. Thermotolerance and synthesis of heat shock proteins: these responses are present in *Hydra attenuata* but absent in *Hydra oligactis*. Proc Natl Acad Sci U S A. 1988;85:7927-7931. https://doi.org/10.1073/pnas.85.21.7927

38. Hofmann GE, Lund SG, Place SP, Whitmer AC. Some like it hot, some like it cold: The HSR is found in New Zealand but not Antarctic notothenioid fishes. J Exp Mar Bio Ecol. 2005;316: 79-89. https://doi.org/10.1016/j.jembe.2004.10.007

39. Clark MS, Fraser KPP, Peck LS. Lack of an HSP70 HSR in two Antarctic marine invertebrates. Polar Biol. 2008;31:1059-1065. https://doi.org/10.1007/s00300-008-0447-7

40. Lindquist S. The Heat-Shock Response. Annu Rev Biochem. 1986;55:1151-1191. https://doi.org/10.1146/annurev.bi.55.070186.005443

41. Nguyen AD, Gotelli NJ, Cahan SH. The evolution of heat shock protein sequences, cis-regulatory elements, and expression profiles in the eusocial Hymenoptera. BMC Evol Biol. 2016;16:15. https://doi.org/10.1186/s12862-015-0573-0

42. Perkins LA, Doctor JS, Zhang K, Stinson L, Perrimon N, Craig EA. Molecular and developmental characterization of the heat shock cognate 4 gene of Drosophila melanogaster. Mol Cell Biol. 1990;10:3232-3238. https://doi.org/10.1128/MCB.10.6.3232

43. Rubin DM, Mehta AD, Zhu J, Shoham S, Chen X, Wells QR et al. Genomic structure and sequence analysis of Drosophila melanogaster HSC70 genes. Gene. 1993;128:155-163. https://doi.org/10.1016/0378-1119(93)90558-k

44. Ribeiro JMC, Arcà B, Lombardo F, Calvo E, Phan VM, Chandra PK et al. An annotated catalogue of salivary gland transcripts in the adult female mosquito, *Aedes aegypti*. BMC Genomics. 2007;8:6. https://doi.org/10.1186/1471-2164-8-6

45. Kapoor M, Curle CA, Runham C. The hsp70 gene family of *Neurospora crassa*: Cloning,

565 sequence analysis, expression, and genetic mapping of the major stress-inducible member. J
566 Bacteriol. 1995;177:212-221. https://doi.org/10.1128/jb.177.1.212-221.1995
567 46. Yost HJ, Lindquist S. Heat shock proteins affect RNA processing during the HSR of
568 *Saccharomyces cerevisiae*. Mol Cell Biol. 1991;11:1062-1068.
569 https://doi.org/10.1128/mcb.11.2.1062
570 47. Evgen'ev MB,·Garbuz DG, Zatsepina OG. Heat shock proteins and whole body adaptation to
571 extreme environments. Dordrecht Heidelberg New York London: Springer; 2014
572 http://dx.doi.org/10.14712/23361964.2015.79
573 48. Stefani RMP, Gomes SL. A unique intron-containing hsp70 gene induced by heat shock and
574 during sporulation in the aquatic fungus *Blastocladiella emersonii*. Gene. 1995;152:19-26.
575 https://doi.org/10.1016/0378-1119(95)00645-M
576 49. Georg RC, Stefani RM, Gomes SL. Environmental stresses inhibit splicing in the aquatic fungus
577 *Blastocladiella emersonii*. BMC Microbiol. 2009;9:231. https://doi.org/10.1186/1471-2180-9-231
578 50. Kummasook A, Pongpom P, Vanittanakom N. Cloning, characterization and differential
579 expression of an hsp70 gene from the pathogenic dimorphic fungus, *Penicillium marneffei*. DNA
580 Seq. 2007;18:385-394. https://doi.org/10.1080/10425170701309012
581 51. Rochester DE, Winer JA, Shah DM. The structure and expression of maize genes encoding the
582 major heat shock protein, hsp70. EMBO J. 1986; 5:451-458.
583 52. Winter J, Wright R, Duck N, Gasser C, Fraley R, Shah D. The inhibition of petunia hsp70 mRNA
584 processing during CdCl2 stress. Mol Gen Genet. 1988;211(2):315-319.
585 https://doi.org/10.1007/BF00330609
586 53. Snutch TP, Heschl MF, Baillie DL. The *Caenorhabditis elegans* hsp70 gene family: a molecular
587 genetic characterization. Gene. 1988; 64(2):241-55. https://doi.org/10.1016/0378-1119(88)90339-
588 3
589 54. Qin W, Tyshenko MG, Wu BS, Walker VK, Robertson RM. Cloning and characterization of a

member of the Hsp70 gene family from *Locusta migratoria*, a highly thermotolerant insect. Cell Stress Chaperones. 2003;8:144-152. https://doi.org/10.1379/1466-1268(2003)008<0144:cacoam>2.0.co;2

55. Huang J, Van der Ploeg. Maturation of polycistronic pre-mRNA in *Trypanosoma brucei*: analysis of trans splicing and poly(A) addition at nascent RNA Transcripts from the *hsp70* locus. Mol Cell Biol. 1991;11(6):3180-90. https://doi.org/10.1128/mcb.11.6.3180

56. Ingolia NT, Lareau LF, Weissman JS. Ribosome profiling of mouse embryonic stem cells reveals the complexity and dynamics of mammalian proteomes. Cell. 2011;147, 789-802. https://doi.org/10.1016/j.cell.2011.10.002.

57. Holcik M, Sonenberg N. Translational control in stress and apoptosis. Nat Rev Mol Cell Biol. 2005 6:318-327. https://doi.org/10.1038/nrm1618

58. Yost HJ, Lindquist S. Translation of unspliced transcripts after heat shock. Science. 1988;242:1544–1548. https://doi.org/10.1126/science.3201243

59. Bond U, James TC. Dynamic changes in small nuclear ribonucleoproteins of heat-stressed and thermotolerant HeLa cells. Int J Biochem Cell Biol. 2000;32:643-656. https://doi.org/10.1016/S1357-2725(00)00008-X

60. Jacob F, Monod J. Genetic regulatory mechanisms in the synthesis of proteins. J Mol Biol. 1961;3:318-356. https://doi.org/10.1016/S0022-2836(61)80072-7

61. Mattick JS, Makunin IV. Non-coding RNA, Human Molecular Genetics. Hum Mol Genet. 2006; 15(1):R17–R29. https://doi.org/10.1093/hmg/ddl046

62. Knigge T, Bachmann L, Köhler H-R. An intron-containing, heat-inducible stress-70 gene in the millipede *Tachypodoiulus niger* (Julidae, Diplopoda). Cell Stress Chaperones. 2014;19:741-747. https://doi.org/10.1007/s12192-014-0494-7

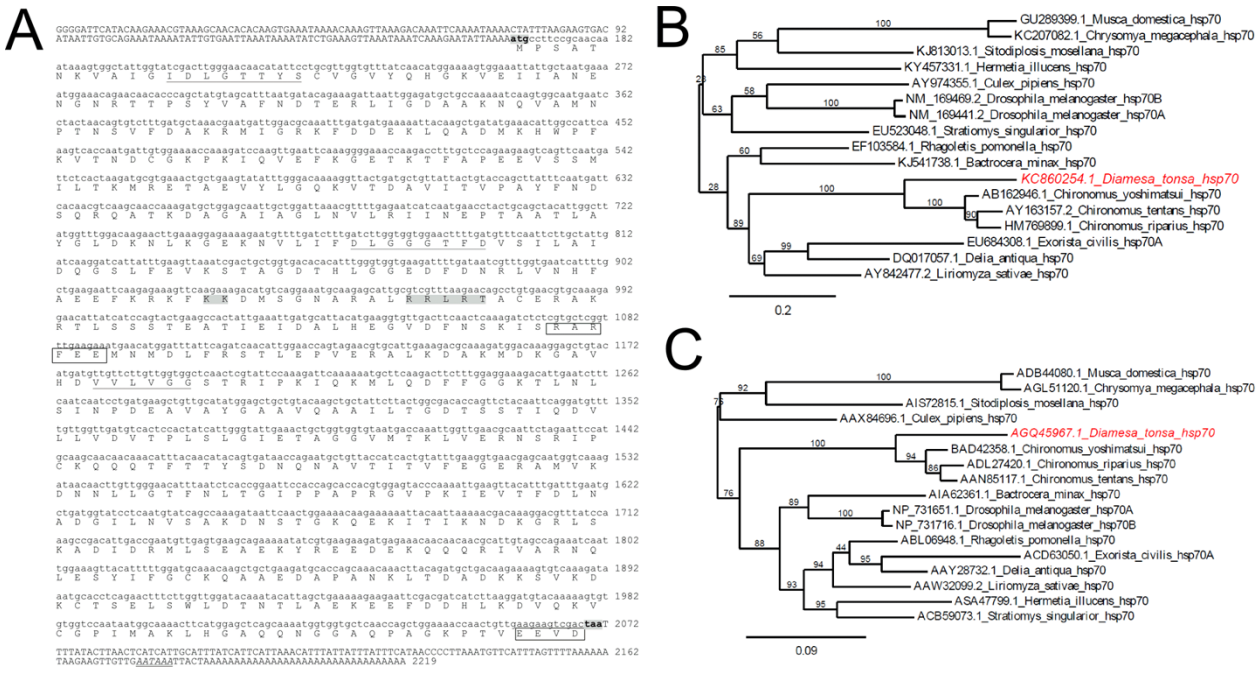

Figure 1. Characterization of *hsp70* gene in *Diamesa tonsa*. (**A**) Nucleotide sequence of the *hsp70* gene in *D. tonsa* with deduced amino acid sequence. In the nucleotide sequence, upper case indicates the 5′UTR and the 3′UTRs, whilst lower case indicates the coding region. The start codon (ATG) and stop codon (TAA) are shadowed and in bold, and the consensus polyA signal in the 3′UTR is in italic and double-underlined. The three characteristic signatures of the HSP70 family are underlined: the non-organelle consensus-motif (RARFEEL) and the cytoplasmic C-terminal region EEVD are shown. The putative bipartite nuclear localization signal (KK and RRLRT) is shadowed in grey. (**B**) Phylogenetic tree inferred from nucleotide sequences of *hsp70* in different dipteran species. The tree was constructed using Phylogeny.fr tool at ExPASy Proteomics server (http://www.phylogeny.fr) using the "One Click" mode with default settings. The numbers above the branches are tree supported values generated by PhyML using the approximate Likelihood Ratio (aLRT) statistical test. (**C**) Phylogenetic tree inferred from the inferred amino-acid sequence of HSP70 in different dipteran species. The tree was constructed using Phylogeny.fr tool at ExPASy Proteomics server (http://www.phylogeny.fr) using the "One Click" mode with default

631 settings. The numbers above the branches are tree supported values generated by PhyML using

632 the approximate Likelihood-Ratio (aLRT) statistical test.

633

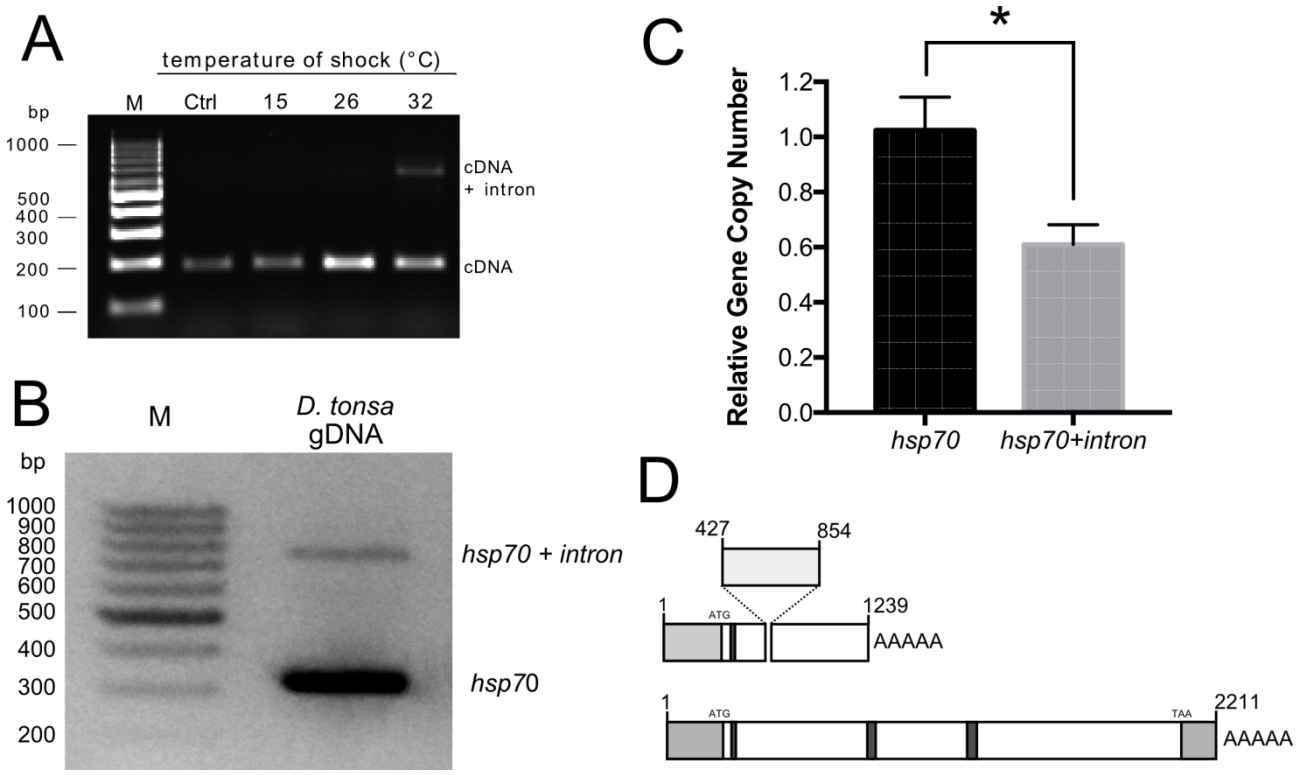

Figure 2. Identification of an Hsp70 pseudogene in *Diamesa tonsa* (**A**) Agarose gel of *hsp70* PCR products from *D. tonsa* larvae control (Ctrl, 4°C) or maintained for 1 h at 15, 26, and 32°C. All PCR products are amplified from cDNA with primers for *hsp70* (**Table 1**). (**B**) Agarose gel electrophoresis of the PCR products amplified from *D. tonsa* genomic DNA with hsp70 sequence specific primers hsp70 F and hsp70 R (**Table 2**). (**C**) Relative gene copy number of hsp70 and hsp70 + intron assessed by Real-PCR analysis (n = 4) (Student *t*-test, * $p \leq 0.05$). (**D**) Schematic representation of the two *hsp70* transcripts: light grey boxes are the 5′ and 3′ UTR, dark grey boxes indicated the position of the three characteristic HSP70 family domains.

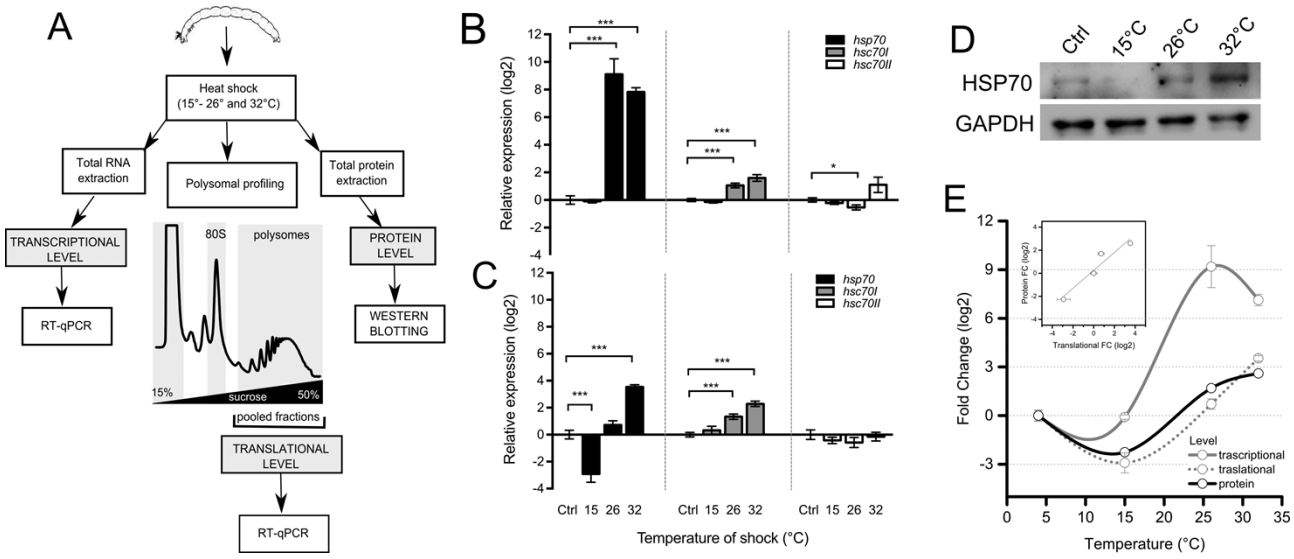

Figure 3. Multi-level analysis of gene expression of *Dc-hsp70*, *hsc70-I* and *hsc70-II* during thermal stress. (**A**) Experimental design for comparing changes in gene expression at multiple levels. Insects were exposed to thermal stress. Total RNA was extracted to analyse the changes at transcriptional level. In parallel, changes associated with mRNA recruitment to polysomes was obtained by RNA extraction from polysomal fractions. These were collected after polysomal profiling to assess the translational changes in gene expression. Finally, whole proteins were extracted to assess protein level. In the first two cases, all three transcripts were studied. For the protein level, only Hsp70 was monitored. (**B**) Transcriptional expression level for *hsp70*, *hsc70-I* and *hsc70-II*. Total RNA was extracted from *Diamesa tonsa* larvae control (Ctrl, 4°C) or maintained for 1 h at 15, 26, and 32°C. *hsp70*, *hsc70-I* and *hsc70-II* relative expression levels were measured by real-time PCR. *Actin* was used as housekeeping gene and the level of control (Ctrl, 4°C) was set at 0. Error bars represent SE; n = 3 biological replicates and each assay was performed in triplicate. (**C**) Translational expression level for *hsp70*, *hsc70-I* and *hsc70-II*. Polysomal RNA was extracted from sucrose fractions corresponding to the polysomal peaks of larvae control (4°C) or maintained for 1 h at 15, 26, and 32°C. *hsp70*, *hsc70-I* and *hsc70-II* relative expression levels were measured by real-time PCR. *Actin* was used as housekeeping gene and the level of control (4°C) was set at 0. (**D**) Western blot analysis of HSP70

protein level in larvae control (Ctrl, 4°C) or maintained for 1 h at 15, 26, and 32°C. GAPDH was used as a loading control. (**E**) Comparison of the $\log_2$ Fold Change with respect to Ctrl of Transcriptional, Translational and Protein level after exposure to 15, 26 and 32°C. Asterisks indicate statistically significant differences with respect to control (Student *t*-test, * $p \leq 0.05$, ** $p \leq 0.01$, *** $p \leq 0.001$). In the inset, the correlation between fold changes occurring at the translational and protein level was calculated (R^2=0.922). In the case of transcriptional and translational comparison, the correlation was (R^2=0.389), see Figure S3A.

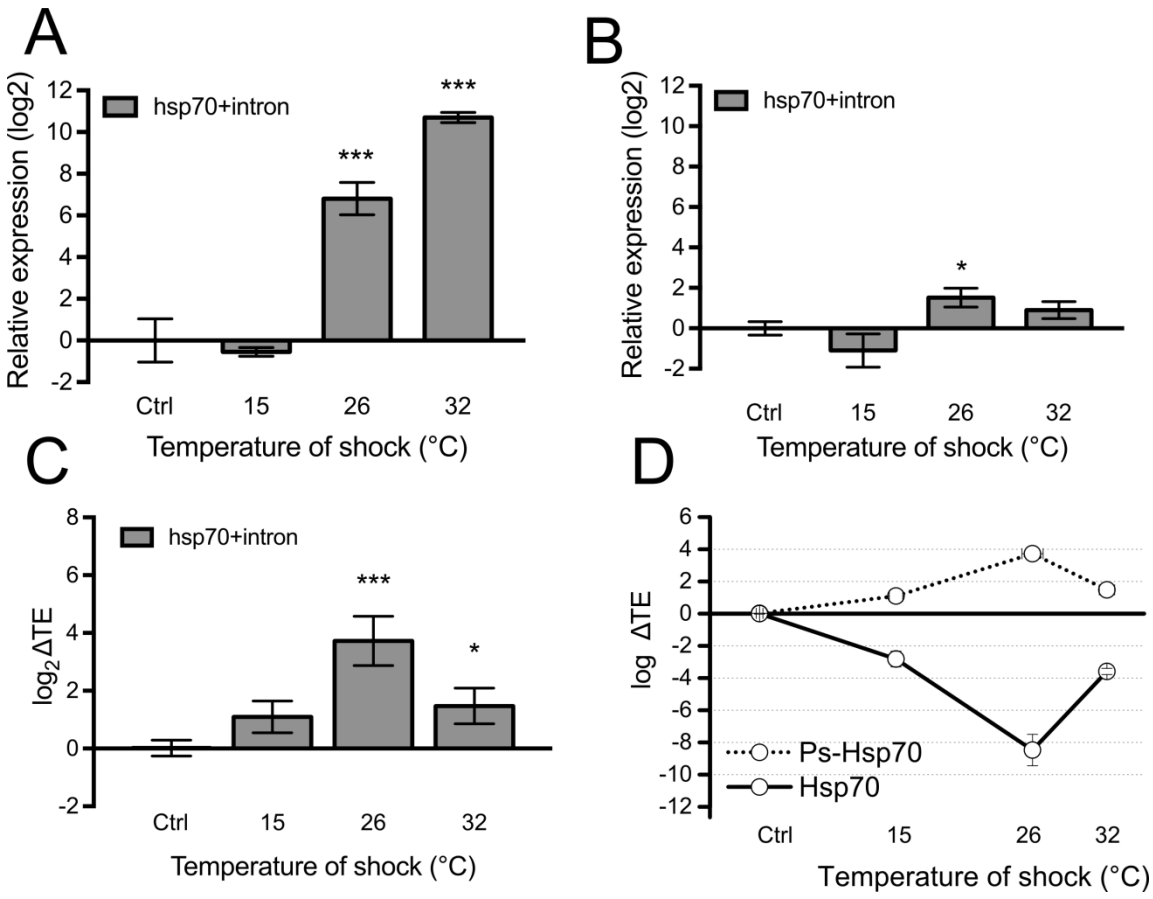

Figure 4 Ps-Hsp70 is loaded on polysomes and acts as a putative ribosome sponge for Hsp70 (**A**) Transcriptional expression level for *hsp70 + intron* mRNA. Total RNA was extracted from *Diamesa tonsa* larvae control (K, 4 °C) or maintained for 1 h at 15, 26, and 32 °C. Relative expression level was measured by real-time PCR. *Actin* was used as housekeeping gene and the level of control (Ctrl, 4 °C) was set at 0. Error bars represent SE; n = 3 biological replicates and each assay performed in triplicate. (**B**) Translational expression level of *hsp70 + intron.* Polysomal RNA was extracted from sucrose fractions corresponding to the polysomal peaks of larvae control (4 °C) or maintained for 1 h at 15, 26, and 32 °C. Relative expression level was measured by real-time PCR. *Actin* was used as housekeeping gene and the level of control (4 °C) was set at 0. (**C**) Translation Efficiency ($\log_2$ ΔTE), calculated as the difference between the fold change at the polysomal level and the fold change at the sub-polysomal level, of *hsp70 + intron* in larvae control (Ctrl, 4 °C) or maintained for 1 h at 15, 26, and 32°C. Asterisks indicate statistically significant differences in respect to the control (Student *t*-test, * $p \leq 0.05$, ** $p \leq 0.01$, *** $p \leq 0.001$). (**D**) Comparison between the Translation Efficiency ($\log_2$ ΔTE) of

685 Ps-Hsp70 and Hsp70. The ΔTE values for Hsp70 were obtained from data shown in Figure 3B and C.

686

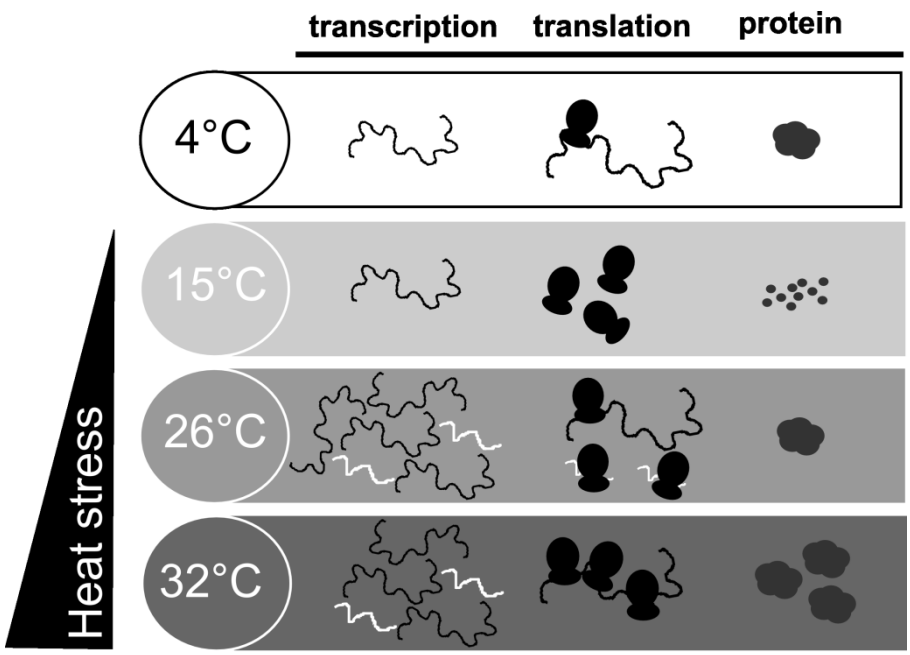

687

688

689 **Figure 5.** Scheme summarizing the multi-level changes occurring during heat shock in *Diamesa tonsa*.

690

691

692

693 **Table 1.** List of primers (5′ -3′) used to amplify *hsp70* with and without intron, *hsc70-I*, *hsc70-II*,

694 and *actin* in RT-PCR analysis.

Primer	*Application*	*Sequence (5′ – 3′)*
Deg_Hsp70-F	5′-3′ RACE PCR	ACVGNTCCNGCNTAYTTYAAYGA
Deg_Hsp70-R	5′-3′ RACE PCR	GCNACNGCYTCRTCNGGRTT
GSP-HSP70_F	5′ RACE PCR	TGATGCAAAGCGGCTGATTGGACGTA
GSP-HSp70_R	3′ RACE PCR	TTGGCAGCATCTCCAATTAATCTTTCTGTATC
GSP-HSC70I_F	5′ RACE PCR	GTCGTAAATTCGATGACCCC
GSP-HSC70I_F	3′ RACE PCR	GACATTACGTTCTCCAGCAG
GSP-HSC70II_F	5′ RACE PCR	GTTTGATCGGTCGTGAATGGAG
GSP-HSC70II_R	3′ RACE PCR	CCCAAATGTGTGTCACCGTTT
Hsp70 Forward	Expression (Fig. 4A)	TTGGGAACAACATATTCCTGC
Hsp70 Reverse	Expression (Fig. 4A)	TTCGTTTAGCATCAAAGACACTG
Hsc70I Forward	qPCR (Fig. 3A/B/C)	GTCGTAAATTCGATGACCCC
Hsc70I Reverse	qPCR (Fig. 3A/B/C)	GACATTACGTTCTCCAGCAG
Hsc70II Forward	qPCR (Fig. 3A/B/C)	GTTTGATCGGTCGTGAATGGAG
Hsc70II Reverse	qPCR (Fig. 3A/B/C)	CCCAAATGTGTGTCACCGTTT
Intron F	qPCR (Fig 4C); CNV (Fig. 5B)	ATGGAGACGCCCAAGAATAA
Intron R	qPCR (Fig 4C); CNV (Fig. 5B)	GTTTTTCTATATCATTCGCACTC
Hsp70 tot F	qPCR (Fig. 3A/B/C; Fig 4C)	TGTTGGAGTTTATCAACATGGA
Hsp70 tot R	qPCR (Fig. 3A/B/C; Fig 4C)	TTTGGCAGCATCTCCAATTA
Hsp70 no intron F	CNV (Fig. 5B)	CAAAAATCAGGTGGCGATGAAT
Hsp70 no intron R	CNV (Fig. 5B)	TGAACTGACTTCTTCTGGAGC
Hsp70 genomic F	gDNA amplification (Fig. 5A)	GAAACAGAACAACACCCAGCT
Hsp70 genomic R	gDNA amplification (Fig. 5A)	ACTTCAGCAGTTTCACGCAT
Actin Forward	qPCR (Fig. 3A/B/C; Fig 4C/D/E/F)	CTGCCTCAACCTCATTGGAAAA
Actin Reverse	qPCR (Fig. 3A/B/C; Fig 4C/D/E/F)	TGGTTGTAGACGGTTTCGTG

695

696

697

698

699 **Table 2.** Summary of the characteristics of all sequences and their deduced proteins (ORF = Open
700 Reading Frame; UTR = Un-Translated Region; tMW = theoretical Molecular Weight).
701

Isoform	***Transcript***					***Protein***		
	Length (nt)	**ORF (nt)**	**5′UTR (nt)**	**3′UTR (nt)**	**polyA**	**Length (aa)**	**tMW (kDa)**	**pI**
Dt-hsp70	2219	1904	166	167	YES	634	69.536	5.67
Dt-hsc70I	2273	1958	121	193	YES	652	71.451	5.47
Dt-hsc70II	2128	1532	410	185	YES	510	56.763	4.95

702
703
704